An Offline Evaluation of the Autoregressive Spectrum for Electrocorticography

Nicholas R. Anderson, Kimberly Wisneski, Lawrence Eisenman, Daniel W. Moran, Eric C. Leuthardt, and Dean J. Krusienski*

***Abstract*—Electrical signals acquired from the cortical surface, or electrocorticography (ECoG), exhibit high spatial and temporal resolution and are valuable for mapping brain activity, detecting irregularities, and controlling a brain–computer interface. As with scalp-recorded EEG, much of the identified information content in ECoG is manifested as amplitude modulations of specific frequency bands. Autoregressive (AR) spectral estimation has proven successful for modeling the well-defined and comparatively limited EEG spectrum. However, because the ECoG spectrum is significantly more extensive with yet undefined dynamics, it cannot be assumed that the ECoG spectrum can be accurately estimated using the same AR model parameters that are valid for analogous EEG studies. This study provides an offline evaluation of AR modeling of ECoG signals for detecting tongue movements. The resulting model parameters can serve as a reference for related AR spectral analysis of ECoG signals.**

***Index Terms*—Autoregressive (AR) spectrum estimation, electrocorticography (ECoG).**

I. Introduction

Autoregressive (AR) modeling is a commonly used technique for spectral estimation of biosignals because it exhibits several advantages over other spectral estimation techniques in this domain; however, its effectiveness is dependent upon proper parameterization [13]. The primary advantage of AR modeling for spectral estimation is its inherent capacity to model the peaky spectra that are characteristic of biosignals. Even so, suitable model order selection for complex biosignals such as EEG, and particularly, electrocorticography (ECoG), is not necessarily straightforward. In order to use AR modeling for estimation and tracking of the ECoG spectrum, it is imperative to determine and validate a suitable model order.

The AR filter is an all-pole model making it very good at resolving sharp changes in the spectra [12]. Conversely, the fast Fourier transformation (FFT) is a widely used nonparametric approach that is very accurate and efficient but lacks spectral resolution for short data segments. The key difference between EEG and ECoG is that ECoG exhibits a much larger functional, spectrum and therefore requires a higher sampling rate [6], [14]. Because of the increased number of samples and added spectral complexity provided by ECoG, it is not appropriate to simply apply a standard AR model order used for EEG to ECoG data.

AR modeling has been used successfully for EEG but has not been evaluated extensively for use with ECoG. Because of its superior resolution for short data segments, AR modeling is preferred for real-time control of an EEG-based brain–computer interface (BCI) [11]. While other ECoG feature extraction techniques have been examined [10], AR modeling continues to be preferred for ECoG motor experiments due to its efficacy for EEG. However, there has been no documented quantification as to how to best choose an appropriate AR model order to accurately model the ECoG dynamics for motor experiments. Recent ECoG motor studies [2]–[9] have implemented AR model orders ranging from 3 to 30.

Typically, the optimal model order of an AR filter is evaluated by assessing the residual error of the model. These computational methods, such as the Akaike information criterion, can provide a reasonable model order in certain contexts. However, these methods are not designed to track signal dynamics and may produce suboptimal estimates for tracking multiple narrow frequency bands. This issue along with other AR model issues for modeling EEG has been evaluated in the context of BCI [15]–[17]. While the issue of AR model order can be easily resolved for EEG due to its well-defined spectral content, much of the relationships and dynamics of the ECoG spectrum have not been characterized. As the AR method becomes more commonplace for tracking the ECoG spectrum, it is imperative to validate the EEG-derived methods demonstrated in initial ECoG studies in order to establish a suitable parameterization and qualify the resulting spectral estimates in this new context.

TABLE I
Individual Subject Results

Subject	A	B	C	D
Age	16	14	46	11
Gender	F	M	F	M
Grid Loc.	Left Temporo-parietal	Left Fronto-parietal	Right Temporo-parietal	Right Fronto-parietal
0-40Hz	0.67 (500/10)	0.37 (500/5)	0.72 (25/FT)	0.35 (500/5)
41-70 Hz	0.82 (500/20)	0.15 (100/FT)	0.82 (100/100)	0.48 (500/10)
71-100 Hz	0.90 (100/FT)	0.26 (500/10)	0.96 (500/10)	**0.66** (500/30)
101-200 Hz	**0.93** (500/90)	**0.93** (500/90)	**0.41** (500/100)	0.42 (25/10)
201-300 Hz	0.78 (500/100)	0.37 (400/90)	0.94 (500/100)	0.12 (300/40)

The age, gender, ECoG grid location, and maximum r^2 ± standard deviation (prior to normalization) in each frequency bin for the four subjects in the study. The model parameters that produced the maximum r^2 are listed below the value as window length in milliseconds/AR model order or "FT" for the FFT). The maximum r^2 achieved by each subject and used for normalization is highlighted in bold.

II. Methodology

A. Data Collection

The subjects in this study were four individuals with intractable epilepsy who underwent temporary placement of intracranial electrode arrays to localize seizure foci prior to surgical resection. All subjects had normal cognition, were right handed, and gave informed consent. The study was approved by the Human Research Protection Organization of Washington University Medical Center. Each subject had a 64-electrode grid placed over the frontal–parietal–temporal region including parts of sensorimotor cortex (refer to Table I). These grids consisted of electrodes with an exposed diameter of 2 mm and an interelectrode distance of 1 cm. Grid placements and duration of ECoG monitoring were based solely on the requirements of the clinical evaluation, without any consideration of this study. Following placement

Manuscript received January 29, 2008; revised May 7, 2008 and August 14, 2008. First published December 2, 2008; current version published April 15, 2009. *Asterisk indicates corresponding author.*

N. R. Anderson, K. Wisneski, and D. W. Moran are with the Department of Biomedical Engineering, Washington University, St. Louis, MO 63130 USA (e-mail: kjw4@cec.wustl.edu; dmoran@wustl.edu).

L. Eisenman is with the Department of Neurology, Washington University, St. Louis, MO 63130 USA.

E. C. Leuthardt is with the Department of Neurological Surgery and Biomedical Engineering, Washington University, St. Louis, MO 63130 USA.

*D. J. Krusienski is with the Department of Electrical Engineering, University of North Florida, Jacksonville, FL 32224 USA (e-mail: deankrusienski@ieee.org).

Digital Object Identifier 10.1109/TBME.2009.2009767

of the subdural grid, each subject had postoperative anterior–posterior and lateral radiographs to verify its location.

Each subject sat in a hospital bed about 75 cm from a video screen. In the experiments, ECoG was recorded from either 16 or 64 electrodes using the general-purpose BCI system BCI2000 [18]. All electrodes were referenced to an inactive electrode, amplified, bandpass filtered (0.5–500 Hz), digitized at 1200 Hz, and stored. The amount of data obtained varied from subject to subject and depended on the subject's physical state and willingness to continue.

For each run, the subject was asked to perform one of two tasks in response to the corresponding visual cue. The two tasks were to protrude the tongue and open and close the hand contralateral to the electrode grid. During a run, the subject continuously repeated the task in response to the visual cue that lasted 3 s (i.e., a trial) and rested for an equal amount of time while the screen was blank between consecutive trials. A total of three 2–3 min runs were performed. These movements versus rest tasks are representative of typical BCI motor screening tasks that are designed to identify potential BCI control signals by localizing differences between the baseline resting state (no movement) and the brain activity resulting from physical movement.

B. Data Processing

For this study, the data from the actual tongue movement and resting intervals were used to evaluate the AR model parameterization. Between 36 and 45 tongue protrusion trials were analyzed for each subject. The parameters of importance include the model order, data segment length, sampling rate, and the desired frequency range. Because the data were originally sampled at 1200 Hz and the AR model order evaluation is very sensitive to the comparatively low signal-to-noise ratio at the higher end of this spectrum, the desired frequency range was selected as 0.5–300 Hz. The AR models were derived via the Burg method [12] and the spectra were computed in 1 Hz bins. The model order was varied from 5 to 100 and data segment length was varied from 25 to 500 ms, with a 16.7 ms overlap. For comparison purposes, the FFT was also computed for the various segment lengths using a Hanning window and zero padding to produce 1 Hz frequency bins.

For both spectral estimation methods, each 1 Hz spectral bin was power normalized using the mean and standard deviation of the respective bin across both conditions (tongue movement versus rest). The power-normalized bins were then averaged into 1–40, 41–70, 71–100, 101–200, and 201–300 Hz composite bins. The normalization was used to compensate for the power-law decay of the ECoG spectrum when averaging across frequency bins so that the inherently larger powers at the lower frequencies do not dominate and artificially skew the averages. For each composite frequency bin, the run average for each task condition was determined and used to compute the r^2 correlation (i.e., the proportion of the variance of the signal accounted for by the task) between the two task conditions.

III. Results

For each subject, the electrode location that produced the highest r^2 for the tongue movement task was selected as optimal. These locations were found to correspond directly to the tongue area of the sensorimotor cortex as verified by radiographs. For each subject's optimal electrode location, the maximum r^2 in each frequency band and the corresponding model parameters that produced these values are provided in Table I.

In order to identify suitable generalized parameters across subjects, for each subject, the r^2 results were normalized to the maximum r^2 (across all frequency bands and parameter combinations) and averaged across subjects. This average normalized r^2 is shown in Fig. 1 and indicates the generalized movement versus rest r^2 correlations produced by the various parameter combinations. Values near 1 indicate that the parameter combination provides a high relative correlation between the resulting feature and the task for all subjects.

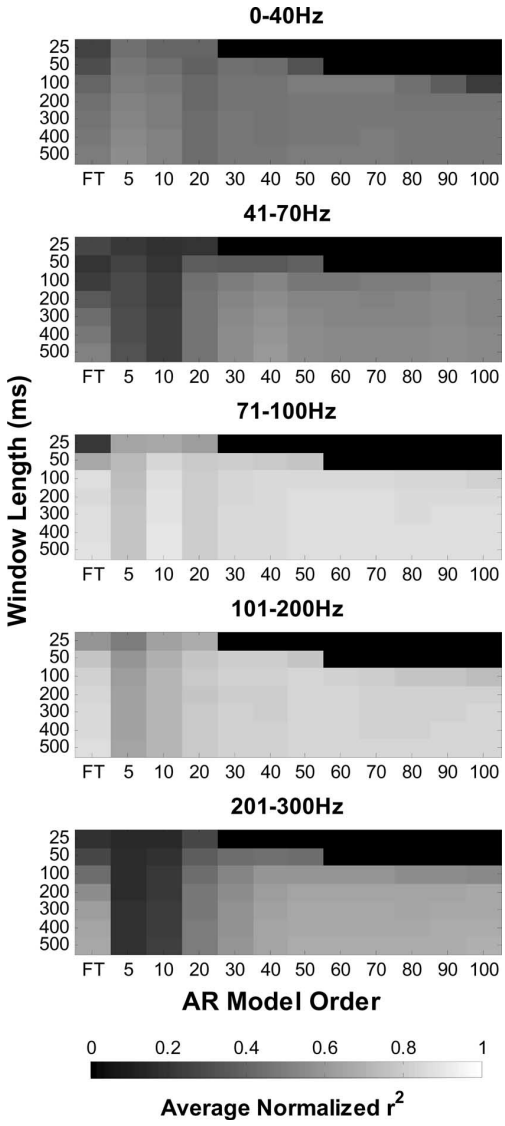

Fig. 1. Generalized tongue movement versus rest r^2 correlations produced by the various parameter combinations of window length and AR model order [including FFT in the first column (FT)]. For each of the four subject's optimal electrode location, the r^2 results were normalized to the maximum r^2 (across all frequency bands and parameter combinations) and averaged across subjects. Values near 1 indicate that the parameter combination provides a high relative correlation between the resulting feature and the task for all subjects.

A repeated measures analysis of variance (ANOVA) was performed on the normalized r^2 results for each frequency bin using *model order*, *window length*, and *user* as factors. Because the shorter window lengths do not produce results for all model orders, which would inaccurately skew the statistics, only window lengths 100–500 ms were used in the ANOVA. The ANOVA indicated significant differences for all factors tested ($p < 0.0001$). The significance of the individual parameters for each factor was evaluated using a *post hoc* Tukey–Kramer test. A window length of 500 ms performed significantly better ($p < 0.05$) than window lengths of 100 and 200 ms for all frequency

TABLE II
TOP AR MODEL ORDERS AND SIGNIFICANT DIFFERENCES

	Top AR Model Order	Significant Differences
0-40Hz	5	FT, 20-100
41-70 Hz	40	FT, 5-20
71-100 Hz	10	All
101-200 Hz	50*	5-30
201-300 Hz	70	FT, 5-40

The top performing AR model orders for each frequency bin and the corresponding significant differences in normalized r^2 as determined by a repeated measures ANOVA and a *post hoc* Tukey – kramer test ($p < 0.05$).
*FT (FFT) marginally outperformed all AR models in this band and was significantly different than 5–30.

bins. The significant differences for model order as determined by the Tukey–Kramer test ($p < 0.05$) for each frequency bin are provided in Table II.

IV. DISCUSSION

The results in Fig. 1 and the statistical analysis indicate a general increase in performance for increasing window sizes, with the 500 ms window clearly providing the best performance. When detection speed is an issue, such as for continuous BCI control applications, the maximum allowable window size should be selected to avoid a compromise in performance. There is not a distinct trend relating window length to model order. The results suggest that the appropriate model order is highly dependent on the frequency band.

The frequency ranges that are commonly used for motor screening and BCI control are 0–40, 71–100z, and 101–200 Hz [6]. Model orders of 5 and 10 appear to best track the dynamics of the two composite low-frequency bands, respectively. This could be due to the fact that comparatively few distinct spectral peaks reside in these ranges, which would correspond to the findings of other EEG and ECoG model order studies [8], [20]. Model orders above 30 appear to be suitable for the 101–200 and 201–300 Hz ranges. This could be due to the fact that these comparatively higher model orders are capable of capturing the more discrete and separable frequency bands associated with distinct physiological processes at the higher frequency ranges [19]. Additionally, it is possible that higher model orders are required for these ranges due to the comparatively lower signal-to-noise ratios.

The 71–200 Hz range shows the maximum r^2 for each subject (Table I) and underscores the potential reliability for ECoG BCI of this frequency band. It is interesting to note that this is the frequency range that has provided good results for ECoG across many studies with different model orders [3], [5]. This indicates that this band may be most neurophysiologically relevant for ECoG. Interestingly, the top AR model performed significantly better than the FFT in all frequency bands except 101–200 Hz, where the FFT performed marginally better. However, the FFT did not yield the highest r^2 for any subject in this band. It is difficult to pinpoint a reason as to why this was the sole range that the FFT results were significantly consistent in comparison to the AR models, but the results support the use of the FFT for this frequency range in Miller *et al.* [9].

Further investigation in this area is necessary to reveal the precise functional relationships and dynamics within the ECoG spectrum. The aforementioned results represent a preliminary analysis and are intended to serve as a starting point for parameterization of AR spectral estimation in ECoG studies. It is anticipated that similar parameters will be adequate for tracking the ECoG spectra from other areas of the sensorimotor cortex; however, additional motor screening data are necessary.

REFERENCES

[1] B. Graimann, J. E. Huggins, S. P. Levine, and G. Pfurtscheller, "Toward a direct brain interface based on human subdural recordings and wavelet-packet analysis," *IEEE Trans. Biomed. Eng.*, vol. 51, no. 6, pp. 954–962, Jun. 2004.

[2] E. A. Felton, J. A. Wilson, J. C. Williams, and C. P. Garell, "Electrocorticographically controlled brain-computer interfaces using motor and sensory imagery in patients with temporary subdural electrode implants. Report of four cases," *J. Neurosurg.*, vol. 106, no. 3, pp. 495–500, 2007.

[3] G. Schalk, J. Kubanek, K. J. Miller, N. R. Anderson, E. C. Leuthardt, J. G. Ojemann, D. Limbrick, D. Moran, L. A. Gerhardt, and J. R. Wolpaw, "Decoding two-dimensional movement trajectories using electrocorticographic signals in humans," *J. Neural Eng.*, vol. 4, pp. 264–275, 2007.

[4] G. Schalk, K. J. Miller, N. R. Anderson, J. A. Wilson, M. D. Smyth, J. G. Ojemann, D. W. Moran, J. R. Wolpaw, and E. C. Leuthardt, "Two-dimensional movement control using electrocorticographic signals in humans," *J. Neural Eng.*, vol. 5, pp. 75–84, 2008.

[5] E. C. Leuthardt, K. J. Miller, G. Schalk, R. N. Rao, and J. G. Ojemann, "Electrocorticography-based brain computer interface—The seattle experience," *IEEE Neural Syst. Rehabil. Eng.*, vol. 14, no. 2, pp. 194–198, Jun. 2006.

[6] E. C. Leuthardt, G. Schalk, J. R. Wolpaw, J. G. Ojemann, and D. W. Moran, "A brain–computer interface using electrocorticographic signals in humans," *J. Neural Eng.*, vol. 1, no. 2, pp. 63–71, 2004.

[7] C. M. Chin, M. R. Popovic, A. Thrasher, T. Cameron, A. Lozano, and R. Chen, "Identification of arm movements using correlation of electrocorticographic spectral components and kinematic recordings," *J. Neural. Eng.*, vol. 4, pp. 146–158, 2007.

[8] T. N. Lal, T. Hinterberger, G. Widman, M. Schröder, J. Hill, W. Rosenstiel, C. E. Elger, B. Schölkopf, and N. Birbaumer, "Methods towards invasive human brain computer interfaces," in *Advances in Neural Information Processing Systems 17*, L. K. Saul, Y. Weiss, and L. Bottou, Eds. Cambridge, MA: MIT Press, 2005, pp. 737–744.

[9] K. J. Miller, E. C. Leuthardt, G. Schalk, R. P. Rao, N. R. Anderson, D. W. Moran, J. W. Miller, and J. G. Ojemann, "Spectral changes in cortical surface potentials during motor movement," *J. Neurosci.*, vol. 27, no. 9, pp. 2424–2432, 2007.

[10] P. M. Shenoy, K. J. Miller, J. G. Ojemann, and R. P. N. Rao, "Generalizable features for electrocorticographic BCIs," *IEEE Trans. Biomed. Eng.*, vol. 55, no. 1, pp. 273–280, Jan. 2008.

[11] J. R. Wolpaw and N. Birbaumer, "Brain-computer interfaces for communication and control," in *Textbook of Neural Repair and Rehabilitation; Neural Repair and Plasticity*, M. E. Selzer, S. Clarke, L. G. Cohen, P. Duncan, F. H. Gage, Eds. Cambridge: Cambridge Univ. Press, 2006, pp. 602–614.

[12] S. L. Marple, *Digital Spectral Analysis With Applications*. Englewood Cliffs, NJ: Prentice-Hall, 1987.

[13] L. H. Zetterberg, "Estimation of parameters for a linear difference equation with application to EEG analysis," *Math. Biosci.*, vol. 5, pp. 227–275, 1969.

[14] D. J. McFarland and J. R. Wolpaw, "EEG-based communication and control: Speed-accuracy relationships," *Appl. Psychophysiol. Biofeedback*, vol. 28, no. 3, pp. 217–231, 2003.

[15] D. J. McFarland and J. R. Wolpaw, "Sensorimotor rhythm-based brain–computer interface (BCI): Model order selection for autoregressive spectral analysis," *J. Neural Eng.*, vol. 5, pp. 155–162, 2008.

[16] D. J. Krusienski, D. J. Mcfarland, and J. R. Wolpaw, "An evaluation of autoregressive spectral estimation model order for brain–computer interface applications," in *Proc. Annu. Int. Conf. IEEE Eng. Med. Biol. Soc.*, 2006, vol. 1, pp. 1323–1326.

[17] F. Babiloni, S. Bufalari, F. Cincotti, M. Marciani, D. Mattia, and M. Mattiocco, "Autoregressive spectral analysis in brain computer interface context," in *Proc. Annu. Int. Conf. IEEE Eng. Med. Biol. Soc.*, 2006, vol. 1, no. 1, pp. 3736–3739.

[18] G. Schalk, D. J. McFarland, T. Hinterberger, N. Birbaumer, and J. R. Wolpaw, "BCI2000: A general-purpose brain–computer interface (BCI) system," *IEEE Trans. Biomed. Eng.*, vol. 51, no. 6, pp. 1034–1043, Jun. 2009.
[19] M. S. Jones, K. D. MacDonald, B. Choi, F. E. Dudek, and D. S. Barth, "Intracellular correlates of fast (>200 Hz) electrical oscillations in rat somatosensory cortex," *J. Neurophysiol.*, vol. 84, pp. 1505–1518, 2000.
[20] F. Vaz, P. Guedes deOliveira, and J. C. Principe, "A study on the best order for autoregressive EEG modelling," *Int. J. Bio-Med. Comput.*, vol. 20, pp. 41–50, 1987.

Resolving Superimposed MUAPs Using Particle Swarm Optimization

Hamid Reza Marateb* and Kevin C. McGill, *Member, IEEE*

***Abstract*—This paper presents an algorithm to resolve superimposed action potentials encountered during the decomposition of electromyographic signals. The algorithm uses particle swarm optimization with a variety of features including randomization, crossover, and multiple swarms. In a simulation study involving realistic superpositions of two to five motor-unit action potentials, the algorithm had an accuracy of 98%.**

***Index Terms*—Alignment, decomposition, electromyography, particle swarm optimization, superposition.**

I. Introduction

The electromyographic (EMG) signal is made up of discharges called motor-unit action potentials (MUAPs). Whenever two or more MUAPs occur within a sufficiently short time interval, their waveforms overlap and superimpose. The problem of identifying the MUAPs involved in a superimposition and finding their precise timing is known as resolving the superimposition [1]–[6]. This problem can be formulated as an optimization problem, namely, that of finding the set of MUAPs templates and their alignment that gives the best match to the superimposition. Finding the solution is challenging because of the large number of possible combinations and alignments and because there are often many local extrema of the objective function.

A simple approach for resolving superimpositions is the peel-off method, in which the MUAPs are successively aligned and subtracted from the superimposition [7]. Unfortunately, the peel-off method often fails to find the optimal solution, especially when the superimposition involves destructive interference. McGill [8] presented an algorithm that finds the optimal solution by discretizing the search space, using a branch-and-bound approach to efficiently find the global discrete-time optimum solution, and then using interpolation to find the nearest continuous-time optimum. Florestal *et al.* [9] presented a probabilistic method that uses a genetic algorithm to explore the search space. In this paper, we present a different probabilistic approach based on particle swarm optimization (PSO). Part of this paper has been presented in an abstract form [10].

Manuscript received April 3, 2008; revised July 12, 2008. First published September 30, 2008; current version published April 15, 2009. This work was supported in part by the Rehabilitation R&D Service of the U.S. Department of Veterans Affairs and in part by the U.S. National Institute of Neurological Disorders and Stroke under Grant 5-R01-NS051507. *Asterisk indicates corresponding author.*

*H. R. Marateb is with the Laboratorio di Ingegneria del Sistema Neuromuscolare (LISiN), Dipartimento di Elettronica, Politecnico di Torino, Turin 10129, Italy (e-mail: hamid.marateb@polito.it).

K. C. McGill is with the Rehabilitation R&D Center, Veterans Affairs (VA) Palo Alto Health Care System, Palo Alto, CA 94304 USA.

Digital Object Identifier 10.1109/TBME.2008.2005953

II. Algorithm

A. Resolution Problem

The resolution problem can be stated as follows. Given a continuous-time waveform $w(t)$ and n continuous templates $s_i(t)$, $i = 1, \ldots, n$, find the offsets $\mathbf{x} = (x_1, \ldots, x_n)$ to minimize the squared error of the residual between the given and reconstructed waveforms

$$f(\mathbf{x}) = \left\| w(t) - \sum_{i=1}^{n} s_i(t - x_i) \right\|^2. \tag{1}$$

Note that x_i can take on noninteger values. This function can be approximated using trigonometric polynomials as follows [8]:

$$f(\mathbf{x}) \approx \tilde{f}(\mathbf{x}) = \sum_{m=-N/2}^{N/2} \left| \tilde{w}_m - \sum_{i=1}^{n} \tilde{s}_{i,m}\, e^{-\frac{j2\pi m x_i}{N}} \right|^2 \tag{2}$$

where $[\tilde{w}_{-N/2}, \ldots, \tilde{w}_{N/2}]$ is the discrete Fourier transform of the sampled signal $[w(0), \ldots, w(N-1)]$, $[\tilde{s}_{i,-N/2}, \ldots, \tilde{s}_{i,N/2}]$ is the discrete Fourier transform of the ith sampled template $[s_i(0), \ldots, s_i(N-1)]$, and all signals are assumed to be sufficiently zero-padded to avoid wraparound difficulties associated with circular time shifts. This is called the "known-constituent" problem since it is assumed that all n templates are involved in the superimposition. In the "unknown-constituent" problem, it is assumed that some subset of the n templates is involved, and the objective is to determine the subset as well as the offsets.

B. Particle Swarm Optimization

PSO is a population-based stochastic optimization algorithm, originally proposed to simulate the social behavior of a flock of birds [11]. PSO is easy to implement and has been successfully applied to a wide range of optimization problems [12]. In this method, each "particle" is a candidate solution that "flies" through the search space. The path of each particle is influenced by its own experience and that of its neighbors. In this paper, the neighborhood of each particle is the entire swarm (star topology) [13].

Each particle i is characterized by these features:

1) $\mathbf{x}_i$: its current position;
2) $\mathbf{v}_i$: its current velocity;
3) $\mathbf{y}_i$: the personal best position it has found;
4) $\hat{\mathbf{y}}_i$: the best position discovered by any of the particles so far.

At each iteration, these features are updated as follows:

$$\mathbf{x}_i^k = \mathbf{x}_i^{k-1} + \mathbf{v}_i^{k-1} \tag{3}$$

$$\mathbf{y}_i^k = \begin{cases} \mathbf{y}_i^{k-1}, & \text{if } f(\mathbf{x}_i^k) \geq f(\mathbf{y}_i^{k-1}) \\ \mathbf{x}_i^k, & \text{if } f(\mathbf{x}_i^k) < f(\mathbf{y}_i^{k-1}) \end{cases} \tag{4}$$

$$\hat{\mathbf{y}}^k \in \left\{ \mathbf{y}_1^k, \ldots, \mathbf{y}_{n_p}^k \right\} | f(\hat{\mathbf{y}}^k) = \min\left(f\left(\mathbf{y}_1^k\right), \ldots f\left(\mathbf{y}_{n_p}^k\right) \right) \tag{5}$$

$$\mathbf{v}_i^k = w\mathbf{v}_i^{k-1} + c_1 \mathbf{r}_1 \bullet (\mathbf{y}_i^k - \mathbf{x}_i^k) + c_2 \mathbf{r}_2 \bullet (\hat{\mathbf{y}}^k - \mathbf{x}_i^k) \tag{6}$$

where $f(\mathbf{x})$ is the objective function, k is the iteration number, n_p is the number of particles in the swarm, and $\bullet$ denotes element-by-element multiplication. The new velocity depends on the previous velocity and the distances of the particle from the personal and neighborhood best positions [13], with the coefficient ω being the inertia weight, c_1 the cognitive acceleration coefficient, c_2 the social acceleration coefficient, and $\mathbf{r}_1$ and $\mathbf{r}_2$ random vectors whose elements are uniformly distributed in $U(0, 1)$. A large value of inertia weight favors global search ("exploration"), while a small value favors local search ("exploitation").